Journal of Macromolecular Science, Part A
Publication details, including instructions for authors and subscription information:
http://www.informaworld.com/smpp/title~content=t713597274

INVESTIGATION OF BIREFRINGENCE AND SURFACE RELIEF GRATING FORMATION IN AZOPOLYMER FILMS

Nirmal K. Viswanathan[a]; Srinivasan Balasubramanian[b]; Jayant Kumar[c]; Sukant K. Tripathy[d]
[a] Optical Communications Technology Center, [b] Center for Advanced Materials, University of Massachusetts—Lowell, Lowell, MA, U.S.A. [c] Department of Physics, University of Massachusetts—Lowell, Lowell, MA, U.S.A. [d] Department of Chemistry, University of Massachusetts—Lowell, Lowell, MA, U.S.A.

Online publication date: 30 November 2001

To cite this Article Viswanathan, Nirmal K. , Balasubramanian, Srinivasan , Kumar, Jayant and Tripathy, Sukant K.(2001) 'INVESTIGATION OF BIREFRINGENCE AND SURFACE RELIEF GRATING FORMATION IN AZOPOLYMER FILMS', Journal of Macromolecular Science, Part A, 38: 12, 1445 — 1462
To link to this Article: DOI: 10.1081/MA-100108397
URL: http://dx.doi.org/10.1081/MA-100108397

J. MACROMOL. SCI.—PURE APPL. CHEM., A38(12), 1445–1462 (2001)

INVESTIGATION OF BIREFRINGENCE AND SURFACE RELIEF GRATING FORMATION IN AZOPOLYMER FILMS

Nirmal K. Viswanathan,[1,3,‡] Srinivasan Balasubramanian,[3] Jayant Kumar,[1,3,*] and Sukant K. Tripathy[2,3,†]

[1]Department of Physics, [2]Department of Chemistry, and
[3]Center for Advanced Materials, University of Massachusetts—Lowell,
Lowell, MA 01854

Dedicated to the memory of Professor Sukant K. Tripathy.

ABSTRACT

Polarization holography is used to study the dynamics of optically induced gratings in azobenzene functionalized polymer films. The simultaneously formed birefringence grating (BG) and surface relief grating (SRG) are investigated by probing the grating formation process with orthogonal linearly polarized beams for different polarization combinations of the writing beams. Our experimental results indicate that for early writing times, vertically polarized beam diffract from the BG while the horizontally polarized beam gets diffracted predominantly from the SRG. Explanation based on the total electric field vector pattern due to interference of polarized beams and its effect on the material gives an insight into the physical processes responsible for the dual-grating formation.

Key Words: Azo polymers; Birefringence; Surface relief gratings

*Corresponding author. E-mail: Jayant_Kumar@uml.edu
‡Current address**:** Optical Communications Technology Center, 3M-Austin
†Deceased.

INTRODUCTION

Azobenzene chromophore containing polymer films belong to a class of photoanisotropic materials, which respond in an unique way to the superposed light interference pattern [1-6]. Thick films (~10 μm) of azobenzene doped polymer systems have been widely studied for birefringence gratings (BG) formed due to spatial variation of both intensity and electric field pattern [7-10]. Since the successful fabrication of large modulation depth (≥ 0.8 μm) surface relief gratings (SRG) in thin (~1 μm) azobenzene chromophore functionalized polymer (referred as azopolymer hereafter) films [11, 12], several research groups have reported the simultaneous formation of both BG and SRG in this class of functionalized polymer films [13-15]. As both the gratings (BG and SRG) are formed simultaneously when an azopolymer film is exposed to interference pattern, it is usually difficult to separate their contribution to the overall diffraction efficiency of the grating [13, 16]. Recently, Labarthet *et al.* [13] and Holme *et al.* [16] have attempted to separate the anisotropic and surface relief phase shifts due to the gratings formed in amorphous and liquid crystalline azopolymer films. As the azopolymer is sensitive to the polarization of the write and read beams, understanding the physical processes responsible for the simultaneous formation of BG and SRG in thin films is essential for fabricating efficient polarization sensitive optical elements (PSOEs) [17, 18].

We have previously reported that SRG formation process in thin azopolymer films strongly depend on the polarization of the writing beams [19-23]. Facile fabrication of SRG in azopolymer film depend on the details of the recording conditions such as the intensity modulation, the spatial variation (in magnitude and direction) of the electric field vector and the presence of a component of electric field gradient in the grating vector direction [21-23]. In this paper, we report the experimental results of monitoring the grating formation process using orthogonal linearly polarized read beams. Our experimental results show that during the a vertically (V-) polarized beam predominantly probes the birefringence grating while the horizontally (H-) polarized read beam probes predominantly the bulk birefringence and surface relief gratings, depending on the polarization combination of the write beams. We first observed that under the most efficient writing condition (example: RCP: LCP), the H- polarized read beam gets diffracted predominantly due to the SRG. Under identical conditions however, the V- polarized read beam probes predominantly the birefringence grating formed in the bulk of the sample until the modulation of the SRG becomes appreciable. The grating formation process was also monitored in transmission with a restricted surface and in reflection. The grating formation monitored in the reflection mode, which primarily measures the growth in the modulation depth of the SRG with V- and H- polarized read beams shows similar behavior until large modulation depths are reached. The ability to distinguish between the two simultaneous processes in the transmission mode is further confirmed by repeating the experiment for different polarization combinations for the writing beams. The observed behavior of the +1 order

diffracted beam intensity is explained based on a model where the phase shifts due to the refractive index and topographic modulations can cancel or add during the grating formation process. Such unique features observed in azopolymer films has been exploited in the fabrication of planar polarization sensitive optical elements including polarization discriminators and polarization beam splitters [24, 25].

Polarization Holography

Interference of two arbitrarily polarized light beams result in the spatial variation of intensity and polarization-state. An azopolymer film exposed to such an optical interference pattern results in the simultaneous formation of bulk birefringence grating and surface relief grating. During grating formation process, the superposed interference pattern photoexcites and reorients the azo molecules due to repeated *trans-cis-trans* photoisomerization process. At the photostationary state the resulting *trans* azo molecules will be oriented predominantly perpendicular to the incident polarization direction [26-28]. For a spatially varying polarization state due to two-beam interference, this process results in a spatially varying orientation of the azo molecules and hence, a birefringence grating (BG). The simultaneous presence of a component of the electric field gradient parallel to the grating vector direction moves the polymer chains resulting in the formation of large modulation-depth surface relief gratings (SRG).

The superposed interference pattern, responsible for the simultaneous formation of the BG and SRG, can vary spatially in both magnitude and direction depending on the polarization of the two interfering beams [5, 6, 23]. This is illustrated in Figure 1 for two p- polarized writing beams with small interference angle. The total polarization state '**P(x)'** is linear but rotates, with linearly varying phase difference, once each grating period. The intensity modulation due to the superposed interference pattern is [29]:

$$I = I_0 + \Delta I \cos(Kx) \tag{1}$$

where I_0 is the intensity of each of the two interfering beams, ΔI the intensity modulation amplitude, a function of the interference angle θ is proportional to $\sin^2\theta$ [23] and $K = (2\pi/\Lambda)$ is the grating vector. The spatially varying electric field vector (in both magnitude and direction) results in a spatially varying refractive index change **'n(x)'** and hence a bulk birefringence grating.[30,31] Assuming linear material response, the spatial variation of the refractive index can be written as:

$$n(x) = n_0 + \Delta n_{ij} \cos(Kx) \tag{2}$$

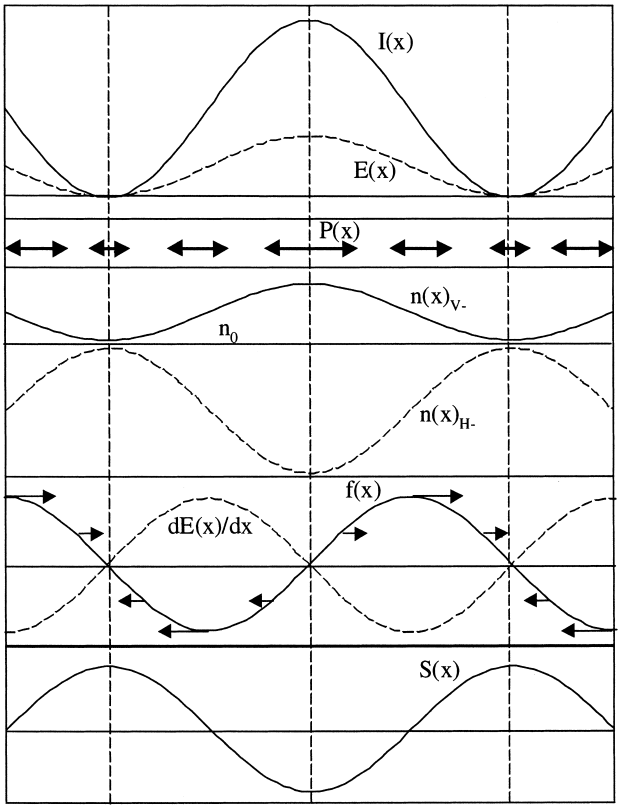

Figure 1. Schematic of the spatial variation of intensity, I(x); electric field, E(x); polarization, P(x) for p-: p- writing beams; refractive index variation, n(x) probed by vertical (V-) and horizontal (H-) polarized beams; gradient of electric field, dE(x)/dx; force, f(x); and the resulting surface modulation, S(x).

where, n_0 is the refractive index of the material before recording (1.63), Δn is the modulated refractive index induced by light induced birefringence. The simultaneous presence of a component of the electric field gradient **'dE(x)/dx'** parallel to the grating vector direction results in a force distribution **'f(x)'** responsible for the large scale polymer chain migration and hence the formation of surface relief profile $S(x) = \Delta S \cos(Kx + \phi)$; where ΔS is the modulation depth of the SRG and ϕ is the arbitrary phase shift of the SRG with respect to the BG.

An experimental investigation to separate the relative contributions of the BG and the SRG is important to completely understand the unique grating formation process in the azopolymer films. Our technique is based on probing the dual grating formation process with orthogonal linearly polarized read beam for different polarization combinations of the write beams. We simplify the treatment by defining the component of the electric field of the read beam $E_{||}$, parallel to the grating grooves (perpendicular grating vector) and the component $E_{\perp}$ to be orthogonal to $E_{||}$. In the Cartesian coordinate system used to investigate the polar-

ization dependent grating formation, $E_{||}$ corresponds to V- polarization and $E_{\perp}$ corresponds to H- polarization. Diffraction efficiency is calculated as a ratio between the diffracted beam intensity (I_d) to the incident beam intensity (I_i) in percentage, i.e., $\eta = (I_d/I_i)$ x100.

The read beam diffracted by a grating in the transmission mode, experiences phase shift due to the induced birefringence given by [29]:

$$\Delta\Phi = \left(2\pi\Delta n\, d/\lambda\right) \tag{3}$$

Simultaneous presence of a large amplitude SRG introduces an additional phase shift of [13, 16]:

$$\Delta\Psi = \left(2\pi n_{eff}\Delta S/\lambda\right) \tag{4}$$

where d is the thickness of the film before irradiation, (0.7 μm) and λ is the read beam wavelength (633 nm). $n_{eff} = (1+n_p)/2$ is the effective refractive index of the SRG with n_p as the refractive index of the azo polymer film (1.68) and assuming $n_{air} = 1$. The effects due to the two phase shifts, observed in the diffracted beam intensity from the gratings [13, 16] can cancel or add depending on the temporal evolution of the Δn and ΔS. Thus, by monitoring the 1st order diffracted beam with orthogonal linearly polarized read beams, it is possible to qualitatively differentiate between the BG and SRG formation processes.

EXPERIMENTAL

The two-beam interferometer setup used in this study is shown in Figure 2. Different polarization combinations for the two interfering Ar^+ laser beams operating at 488 nm can be configured by appropriately orienting the polarizers and polarization rotators (λ/2 and λ/4 waveplates) inserted in the beam path. A polarized He-Ne laser beam (633 nm) is used to read the grating formation process for all the different polarization combinations of the writing beams. The polarization state of the read beam can be changed between V- and H- by rotating the λ/2 waveplate accordingly. The first order diffracted beam intensity is monitored in all the measurements unless specified otherwise. The angle between the two interfering beams (θ) and the writing beam intensity are kept fixed at ≈14° (for a grating periodicity of Λ ≈ 1 μm) and at 50 mW/cm^2 respectively for all the recordings.

The azobenzene functionalized polymer used in this study, CH-1A-CA, is an epoxy based amorphous polymer synthesized by post-azo coupling reaction [32, 33]. The number average molecular weight of the polymer is 5,000 g/mol and its T_g is 93°C. The azopolymer is dissolved in DMF, spin coated on clean glass slide and vacuum dried for 12 hours to obtain good optical quality films. By measuring the refractive index and thickness of the film at different places, using a prism

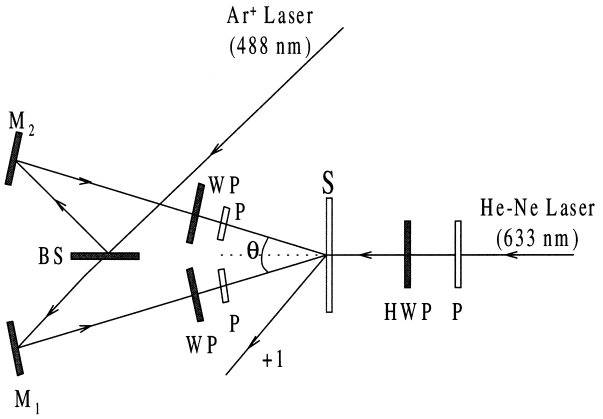

Figure 2. Experimental setup used in this study.

coupler (Metricon 2010), it is made certain that the polymer film is uniform over the entire sample area. The average thickness and refractive index of the film measured at 633 nm are 0.7 μm and 1.68, respectively. The SRGs are scanned using an atomic force microscope (AFM, Cp, Park Scientific, Sunnyvale CA) in the contact mode with SiN cantilever.

RESULTS AND DISCUSSION

The polarization combinations for the writing beams are grouped according to the modulation depth of the SRG fabricated on the azopolymer film due to the superposed interference pattern. Writing beam polarization combinations s-: s-; s-: p-; +45°: +45° and RCP: RCP belong to the first category where modulation depth of the SRG is small (≤ 200 Å) and p-: p-, +45°: -45° and RCP: LCP where large modulation depth SRGs (≥ 1000 Å) can be fabricated belong to the second category.

During the grating formation process we first observed that the diffraction efficiency of the grating depends strongly on the polarization of the read beam. The situation where efficient BG and SRG are simultaneously formed (specifically, RCP: LCP, Figure 3) the diffracted intensity due to V- polarized read beam increases almost instantaneously and saturates in less than 100 seconds typical of the bulk birefringence grating. An AFM scan of polymer film surface after stopping the grating formation at 100 seconds shows no significant SRG. After the initial increase, $\eta_{\|}$ probed by the V- polarized read beam remains saturated until 600 seconds due to saturation in the net orientation of *trans* azo molecules in the sample plane. However, the diffracted intensity due to H- polarized read beam increases almost linearly due to increasing modulation depth of the SRG, confirmed through an independent study. As the modulation depth of the SRG continues to increase, the diffraction efficiency due to V- polarized read beam starts to

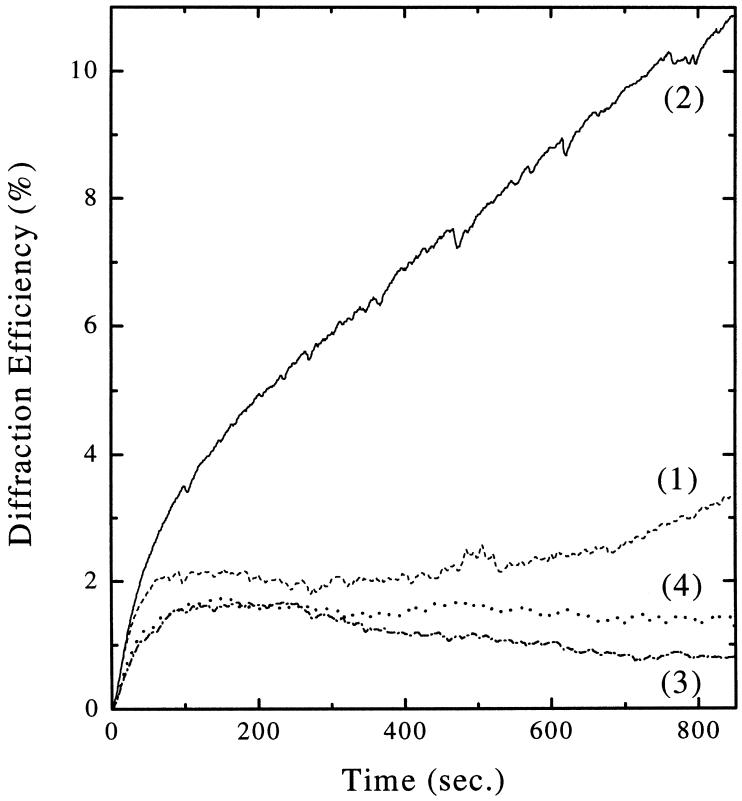

Figure 3. Diffraction efficiency as a function of time for the RCP: LCP writing beam combination. The grating formation is monitored by V- and H- polarized read beams for unrestricted and restricted surfaces: (1) read beam: V-; unrestricted surface; (2) read beam: H-; unrestricted surface; (3) read beam: V-; restricted surface; (4) read beam: H-; restricted surface.

increase. A surface modulation depth of 850 Å was measured after stopping the grating formation process at 700 seconds.

Figure 3 also shows the dynamics of the grating formation in azopolymer film with restricted surface. By covering the azo polymer film with a drop of water and a glass slide, the free surface was severely restricted. This is expected to inhibit only the surface movement and hence the SRG formation process and uninhibited formation of bulk birefringence grating [21, 34]. It can be seen from Figure 3 that an initial increase in the diffracted beam intensity due predominantly to the bulk birefringence grating is still formed. However, the value remains saturated until the end of the recording for both (V- and H-) read beam polarizations. The small difference in the diffracted beam intensities towards the end of the recording is due to a weak surface relief grating, confirmed by an AFM scan to have a maximum modulation depth of 100 Å. Next, we monitored the diffracted beam intensity in the reflection mode with V- and H- polarized read beams to measure the behavior due to SRG without probing any appreciable birefringence

contributions. The diffracted beam from surface reflection primarily senses the growth of the surface modulation depth of the grating without probing significantly effects from the index changes in the material [24]. As before the grating is written with RCP: LCP polarization combination for the write beams. The diffracted beam intensity shows an almost linear increase for both V- and H- polarized read beams till large modulation depth for the SRG is reached (Figure 4). This behavior is markedly different from the behavior of the diffraction efficiency obtained in transmission. Stopping the grating formation process at 1500 seconds, where an appreciable difference between $\eta_{\parallel}$ and $\eta_{\perp}$ starts to appear, a modulation depth of 1100 Å for the SRG was measured. Continuing the recording further increases the modulation depth of the SRG with an enhanced difference between the V- and H- polarized diffracted beam intensities. The diffracted beam intensity due to the surface modulation development saturates at 2500 sec. The corresponding modulation depth of the SRG measured by an AFM scan is 2600 Å. The diffraction efficiency due to the large modulation depth SRG, is more for the V-polarized read beam than for the H- polarized read beam i.e., $\eta_{\parallel} > \eta_{\perp}$.

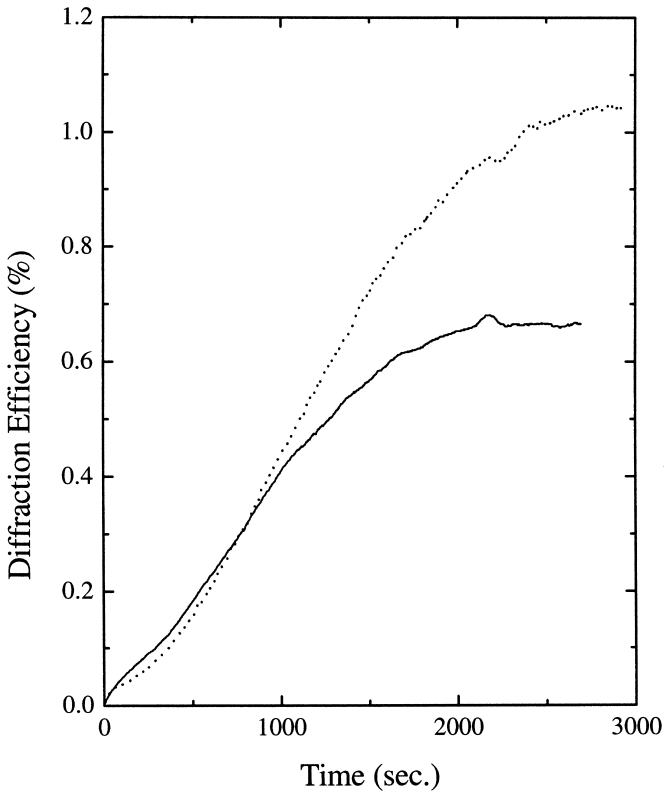

Figure 4. Diffraction efficiency as a function of time for RCP: LCP writing beam combination. The grating formation is monitored in the +1 reflected order. Dotted line is for the V- polarized read beam and continuous line is for the H- polarized read beam.

We wrote gratings in azopolymer film for different polarization combinations of write beams while probing with orthogonally polarized read beams. The spatial variation of the total electric field vector in the sample plane due to interference of two beams of same polarization state, i.e., s-: s-; p-: p-; +45°: +45° and RCP: RCP, varies only in its magnitude, preserving its direction. However, for orthogonal polarization combinations for the interfering beams (s-: p-; +45°: -45° and RCP: LCP) the spatial variation of the electric field vector is both in magnitude and direction. The periodicity of the spatial variation of the electric field vector depends on the phase difference ($\Phi_{12} = 2\pi x/\Lambda$) between the interfering beams. The experimental results and discussion is separated into two groups based on the effects the spatial variation of the electric field vector pattern has on azopolymer film. In the first category, the diffracted beam intensity is predominantly due to the birefringence grating with a weak SRG (≤ 150 Å) while the large modulation depth (> 1000 Å) surface relief gratings dominate the diffraction efficiency in the second category.

Weak SRG

When both the interfering beams are s- polarized, the resulting electric field vector is parallel to s- (inset in Figure 5-a) with maximum intensity modulation ($\Delta I = 4$) [23]. The behavior of the diffracted beam intensity monitored by the V-polarized (dotted line) and the H- polarized (continuous line) read beams are shown in Figure 5-a. The initial increase in the diffracted beam intensity is more for the H- polarized read beam than for the V- polarized read beam. The *trans-cis-trans* photoisomerization process and associated reorientation of the azo molecules orthogonal to the local polarization direction results in a transient increase in the diffraction efficiency for the H-polarized read beam more than that due to the V-polarized read beam. However, finally (after 500 seconds) the spatially varying electric field vector pattern and intensity modulation results in a photostationary state when the Δn due to photoinduced birefringence and hence the diffraction efficiency approach zero. There is little distinction between the two diffracted intensities. The recorded diffraction efficiency for the V- and H- polarization alternate for continued exposure due to complex material response, which is not clear at this time. An AFM scan of the exposed region shows weak surface relief feature of < 100 Å modulation depth.

Interference of orthogonal linearly polarized light beams (s-: p-), results in a pure spatial variation of the electric field vector direction (inset of Figure 5-b) with zero intensity modulation ($\Delta I = 0$) across the interference region [6, 23]. The azopolymer film exposed to this interference pattern results in a higher diffraction efficiency for H- polarized read beam as compared to the V- polarized beam (Figure 5-b). AFM scan of the exposed region at the end of the recording shows a weak SRG with a maximum modulation depth of 200 Å. In addition, the inscribed

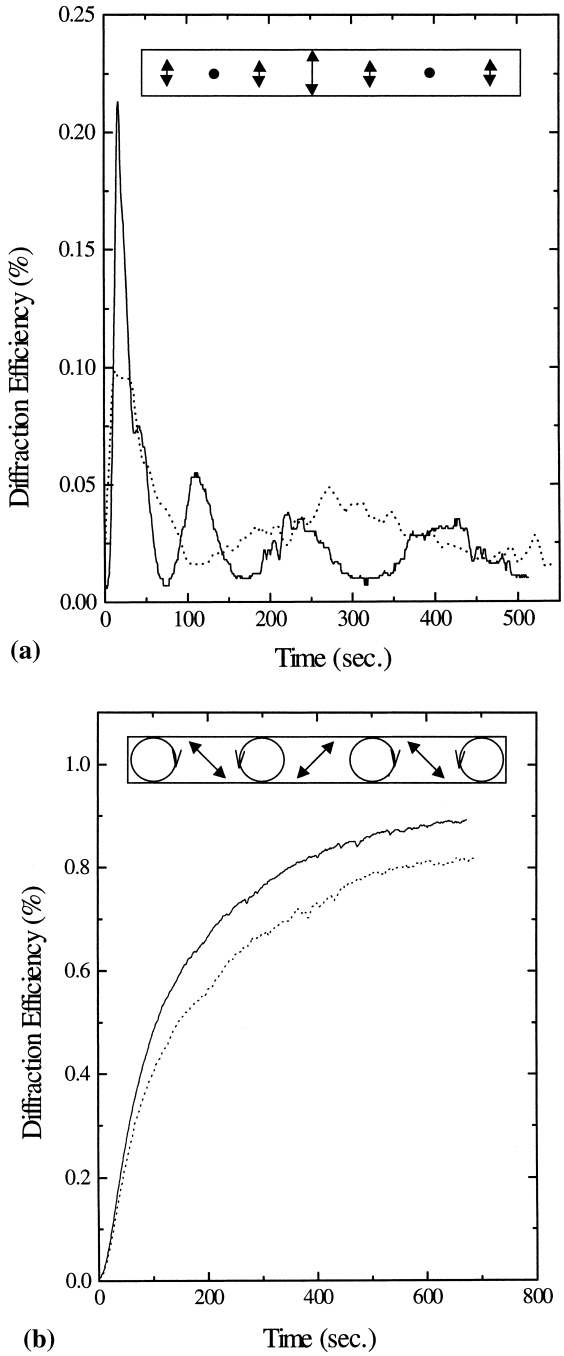

Figure 5. Diffraction efficiency as a function of time for different polarization combinations for the writing beams. The grating formation is monitored in the +1 transmitted order. Dotted line: V- polarized read beam and continuous line: H- polarized read beam. Inset shows the interference field distribution. (a) s-: s-; (b) s-: p-; (c) +45°: +45°; (d) RCP: RCP; (e) p-: p-; (f) +45°: -45°; (g) RCP: LCP.

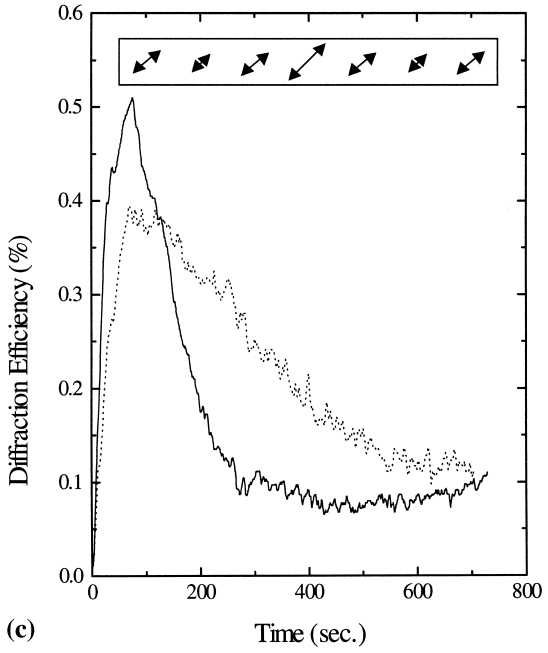

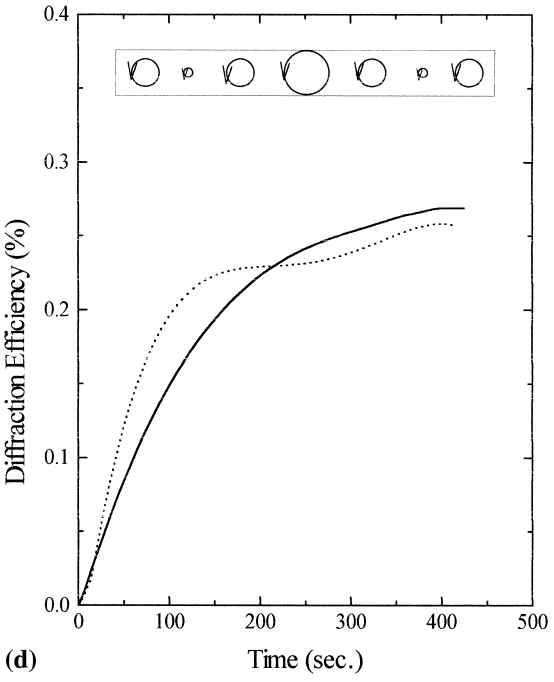

Figure 5. Continued.

(*continued*)

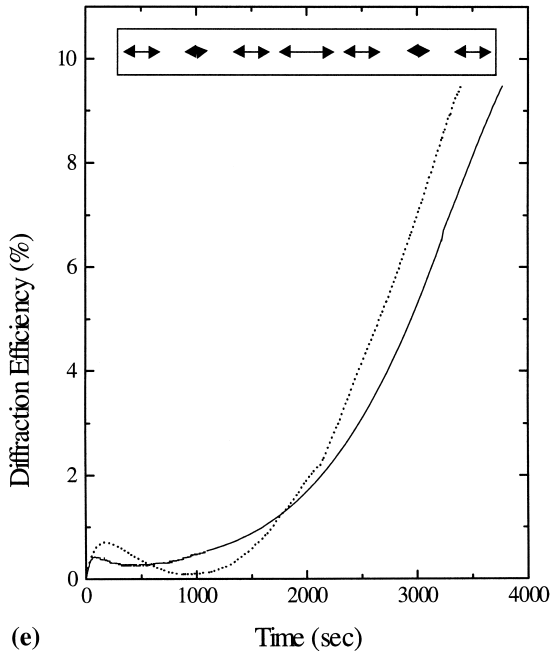

(e)

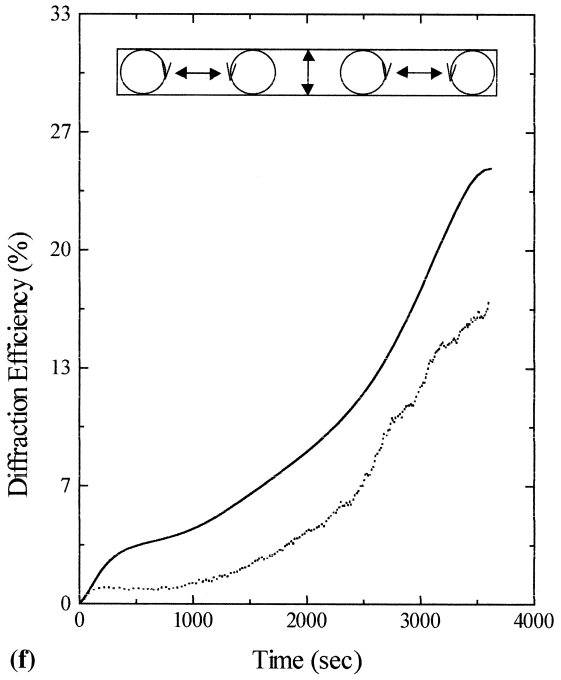

(f)

Figure 5. Continued.

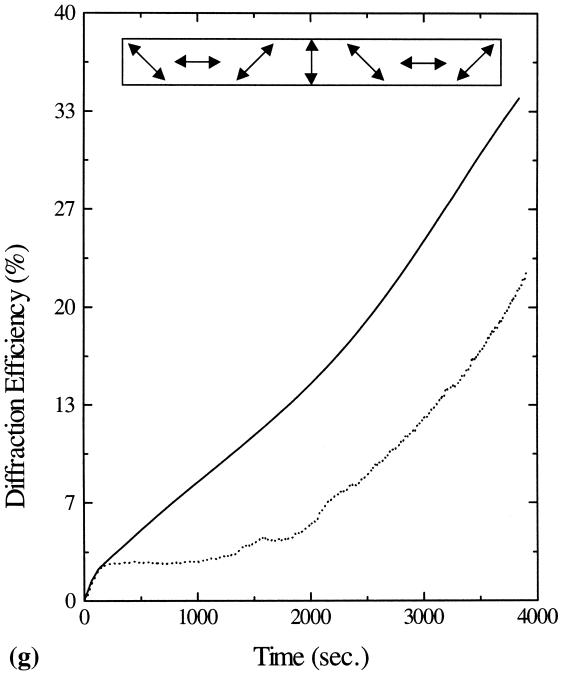

Figure 5. Continued.

birefringence grating is larger and takes longer time to saturate due to the spatial variation of electric field vector pattern [23].

Interference of linearly polarized beams at +45°: +45° results in the spatial variation of the magnitude of the electric field vector with its direction fixed at +45° [23] (inset of Figure 5-c). Monitoring the grating formation with V- and H-polarized read beams results in a behavior shown in Figure 5-c. The initial increase in the diffracted beam intensity due to the photoinduced birefringence grating is more for the H- polarized read beam. However, continuing the recording shows a decrease in the diffracted beam intensity to almost zero and at the end of the recording there is no appreciable difference between the two. As the direction of the electric field vector over the exposed region is the same (+45°), the Δn due to photoinduced birefringence grating and hence, the diffraction efficiency approach zero in the photostationary state. Exposed region shows a weak surface relief feature with modulation depth < 100 Å in an AFM scan. Similar behavior is observed for the -45°: -45° writing configuration also.

RCP: RCP polarization combination for the interfering beams also results in the spatial variation of the magnitude of the electric field vector but with constant direction (parallel to the RCP direction; inset of Figure 5-d) [23]. Figure 5-d shows the diffraction efficiency of the grating as a function of time for both V- and H- polarized read beams. Initial increase in the diffracted beam intensity due to the birefringence grating remains saturated at the maximum value until the end of

the recording. Though the time development of the two curves appears similar, the diffraction efficiency $\eta_{\perp}$ is slightly more than $\eta_{||}$. An AFM scan of the exposed region shows a maximum surface modulation depth of ~100 Å. Similar behavior is observed when the experiment is repeated for the LCP: LCP writing configuration.

Strong SRG

When the response of azopolymer film is exposed to the spatial variation of electric field vector due to p-: p-, +45°: -45° and RCP: LCP writing beam polarization combinations efficient and large modulation depth (> 1000 Å) SRGs are formed [23]. However, the simultaneous presence of birefringence grating depends on the individual cases as will be discussed in the following paragraphs.

When both the writing beams are p- polarized, the electric field vector varies spatially in magnitude resulting in an intensity modulation, which depends on the angle of interference [23]. The electric field vector direction is parallel to the write beam polarization in the X-Y plane and the spatial variation in the X-Z plane results in photoisomerization cycling of the azo molecules. As discussed earlier, [23] the simultaneous presence of spatial variation of the magnitude and direction of the electric field vector pattern in addition to the electric field gradient parallel to the grating vector direction results in the formation of efficient SRGs. Figure 5-e shows the time development of the diffraction efficiency due to V- and H- polarized read beams for the p-: p- writing condition.

The situation is different while recording the grating with +45°: -45° and RCP: LCP writing beam polarization combinations. In these two cases, it is important to note that $\Delta I = 0$ only when $\theta = 0$. In other words, though the two interfering beams are polarized in the opposite sense, the resulting intensity pattern varies spatially when the interference angle is greater than zero. This, along with the spatial variation in the electric field vector direction (inset of Figures 5-f and 5-g) and a component of field gradient parallel to the grating vector in the sample plane results in the simultaneous formation of BG and SRG. As can be seen from Figure 5-f and 5-g, the initial increase in the diffraction efficiency due to V- polarized read beam remains saturated till ~1000 seconds characteristic of the birefringence grating and continues to increase thereafter. The initial increase due to the birefringence grating probed by H- polarized read beam is similar to that with the V- polarized read beam. However, the diffracted beam intensity due to H- polarized read beam probing predominantly the SRG formation continues to increase without any saturated behavior until large diffraction efficiencies are achieved.

It is clear from Figure 2 that the diffraction efficiency monitored in transmission shows a dramatically different behavior for the V- and H- polarized read beams. However, the diffraction efficiency of the same grating monitored in

reflection for both V- and H- polarized read beams are essentially the same until ~1000 seconds (Figure 3). These experimental results clearly suggest that the bulk birefringence grating has different effects in transmission and reflection for the V- and H- polarized read beams. Also, for the azopolymer film with restricted surface, the diffraction efficiency due to both V- and H- polarized read beams result in similar behavior with time, as one would expect in the absence of a SRG.

The experimental results presented above, where a weak SRG is formed on the azopolymer film due to s-: s-; s-: p-; +45°: +45° and RCP: RCP polarization combinations for the two interfering beams can be summarized as follows. The weak SRG in azopolymer film is formed under two writing conditions. (1) The magnitude of the electric field vector varies spatially while its direction remains the same, (as the writing beam polarization) as in s-: s-; +45°: +45° and RCP: RCP or (2) the direction of the electric field vector varies spatially while its magnitude remains constant as in s-: p-. The photoinduced birefringence grating under both of the above mentioned situations has varied effects on the diffraction efficiency due to V- and H- polarized read beams, resulting in a noticeable difference in their behavior. However, when the photostationary state is reached, the spatial variation of index almost and so does the difference between the diffracted beam intensities probed by the V- and H- polarized read beams. This is clearly seen in the recordings for the grating formation as a function of time for the above mentioned cases (Figures 5-a, b, c and d). In these cases, a small difference in the diffraction efficiency due to V- and H- polarized read beams is attributed to ≤100 Å modulation depth of the SRG formed.

Interference of two p- polarized beam results in a field vector distribution in the sample plane parallel to the p- direction (inset of Figure 5-e). Also, temporally the phase relationship between fields diffracted by the BG and SRG change. As the surface becomes increasingly deformed, the bulk grating may reconfigure itself so that the phase relationships at earlier times may be different than later times. The diffraction efficiency for p- polarized writing indicates this. Initially, V-polarized read beam has higher diffraction efficiency compared to H-. At about 1000 seconds, the V- polarized read beam has almost zero diffraction efficiency and finally at times longer than 2000 seconds, V- polarized read beam has a higher diffraction efficiency than the H- beam. The situations where the surface relief grating is small i.e., s-: s-, s-: p-, +45°: -45° and RCP: RCP there is not such a dramatic difference between the behavior of V- and H- polarized read beams. However, in these cases because of the presence of a non-zero (but weak) SRGs, there may be a much smaller effect related to the relative phases of the fields diffracted by V- and H- polarized read beams.

This effect is also dramatically seen when the grating is written with the +45°: -45° and RCP: LCP writing beam polarization. The field vector distribution in the sample plane (inset of Figures 5-f and 5-g) results in a similar behavior for the birefringence grating probed by the V- and H- polarized read beams. However, once the surface of the azopolymer films starts to get modified significantly, the

diffracted beam intensity probed by the H- polarized read beam grows rapidly. Such a behavior can be explained as follows. In these two cases, the position where maximum birefringence is induced ($\Phi_{12} = 0$) is the place where the material is piled up resulting in a surface maximum. This corresponds to the situation where there is no phase difference between the birefringence and surface relief maxima i.e., $\phi = 0$. Thus, we record a continued increase in the diffracted beam intensity for the H- polarized read beam. In addition, as the modulation depth of the SRG formed becomes appreciable, the difference in the diffraction efficiency between the V- and H- polarized read beams become smaller. This can be seen from the increase in the diffracted beam intensity due to V- polarized read beam and its behavior appears similar to that with the H- polarized read beam. By stopping the recording at 1500 seconds, we measured a modulation depth of 830 Å and 1100 Å, respectively for the +45°: -45° and RCP: LCP configurations.

Comparing all the three cases discussed above, we find that the SRG formation rate in the p-: p- case is slower compared to the +45°: -45° and RCP: LCP writing polarization combinations. In the p-: p- case, the electric field vector pattern in the sample plane is parallel to the p- direction and varies only in its magnitude. In the other two cases, the direction of the electric field vector varies spatially across the interference region along with a variation in its magnitude when $\theta > 0°$. Consequently, in the p-: p- case, once the azo molecules in the sample plane have undergone photoinduced reorientation due to repeated *trans-cis-trans* isomerization cycle, the material, for all practical purposes can be thought to be isotropic in the plane. However, the field distribution in the XZ plane helps in continued cycling of the molecules once the free surface starts to get deformed and is responsible for the continued increase of the SRG modulation depths.[23] This is a plausible reason for the slow SRG formation rate compared to the other two cases.

CONCLUSION

We have investigated the simultaneous formation of birefringence grating and surface relief grating formation processes in azopolymer films using polarization holography. We have observed that there is a marked difference in the diffraction efficiency probed by V- and H- polarized read beams from the simultaneous BG and SRG formation. Experimental measurements with unrestricted and restricted surfaces in the transmission and reflection modes demonstrates that the V- polarized read beam is predominantly diffracted from the BG while the SRG predominantly diffracts the H- polarized read beam. Repeating the experiment for different polarization combinations of the writing beams and analyzing the results based on the electric field vector pattern due to interference gives a qualitative understanding of the physical processes responsible for recording BG and SRG in azopolymer films. Further, this study extends the scope of the gratings fabricated on azopolymer films for a variety of polarization sensitive applications.

ACKNOWLEDGMENT

Financial support from the Office of Naval Research (ONR) and National Science Foundation - Division of Materials Research (NSF-DMR) are gratefully acknowledged.

REFERENCES

1. Todorov, T.; Nikolova, L.; Tomova, N. Appl. Opt., **1984**, *23,* 4309.
2. Todorov, T.; Nikolova, L.; Tomova, N. Appl. Opt. **1984**, *23*, 4588.
3. Nikolova, L; Todorov, T. Opt. Acta., **1984**, *5*, 579.
4. Kakichashivili, Sh.D. ; Kilosanidze, B.N. Opt. Spectrosc., **1988**, *65*, 243.
5. Huang, T.; Wagner, K.H. IEEE J. Quant. Electron., **1995**, *13*, 1317.
6. Huang, T.; Wagner, K.H. J. Opt. Soc. Am. B, **1996**, *13*, 282.
7. Couture, J.J.A.; Lessard, R.A. Appl. Opt. **1988**, *27*, 3368.
8. Shi, Y.; Steier, W.H.; Yu, L.; Chen, M.; Dalton, L. Appl. Phys. Lett. **1991**, *59,* 2935.
9. Rochon, P.; Gosselin, J.; Natansohn, A.; Xie, S. Appl. Phys. Lett., **1992**, *60*, 6.
10. Wang, C.; Fei, H.; Yang, Y.; Wei, Z.; Qiu, Y.; Chen, Y. Opt. Commun., **1999**, *159*, 58.
11. Rochon, P.; Batalla, E.; Natansohn, A. Appl. Phys. Lett., **1995**, *66*, 136.
12. Kim, D.Y.; Tripathy, S.K.; Li, L. J. Kumar, Appl. Phys. Lett., **1995**, *66*, 1166.
13. Labarthet, F.L.; Buffeteau, T.; Sourisseau, C. J. Chem. Phys. B, **1998**, *102*, 2654.
14. Lefin, P.; Fiorini, C.; Nunzi, J.M. Opt. Mater., **1998**, *9*, 323.
15. Darracq, B.; Chaput, F.; Lahlil, K.; Levy, Y.; Boilot, J.P. Adv. Mater., **1998**, *10*, 1133.
16. Holme, N.C.R.; Nikolova, L.; Ramanujam, P.S.; Hvilsted, S. Appl. Phys. Lett., **1997**, *70*, 1518.
17. Butler, J.J.; Rodriguez, M.A.; Malcuit, M.S.; Stone, T.W. Opt. Commun., **1998**, *155*, 23.
18. Madamopoulos, N.; Riza, N.A. Opt. Commun. **1998**, *157*, 225.
19. Kim, D.Y.; Li, L.; Jiang, X.L.; Shivshankar, V.; Kumar, J.; Tripathy, S.K. Macromolecules **1995**, *28*, 2618.
20. Jiang, X.L.; Li, L.; Kumar, J.; Kim, D.Y.; Tripathy, S.K. Appl. Phys. Lett., **1995**, *68*, 2618.
21. Kumar, J.; Li, L.; Jiang, X.L.; Kim, D.Y.; Lee, T.S.; Tripathy, S.K. Appl. Phys. Lett., **1998**, *72*, 2096.
22. Bian, S.; Li, L.; Kumar, J.; Kim, D.Y.; Williams, J.; Tripathy, S.K. Appl. Phys. Lett., **1998**, *73*, 1817.
23. Viswanathan, N.K.; Balasubramanian, S.; Li, L.; Kumar, J.; Tripathy, S.K. Jpn. J. Appl. Phys., **1999**, *38*, 5928.
24. Haidner, H.; Kipfer, P.; Sheridan, J.T.; Schwider, J.; Streibl, N.; Lindolf, J.; Collischon, M.; Lang, A.; Hutfless, J. Opt. Eng., **1993**, *32*, 1860.
25. Viswanathan, N.K.; Balasubramanian, S.; Kumar, J.; Tripathy, S.K. Polym. Adv. Technol., **2000**, *11*, 570.
26. Rau, H. "Photoisomerization of Azobenzenes," in Photochemistry and Photophysics, Rabeck, F.J., Ed., CRC Press: Boca Raton, FL; 1990, Vol. 2, Ch. 4, pp. 119-141.
27. Sekkat, Z.; Morichere, D.; Dumont, M.; Saibi, R.L.; Delaire, J.A. J. Appl. Phys., **1992**, *71,* 1543.

28. Sekkat, Z.; Wood, J.; Aust, E.F.; Knoll, W.; Volksen, W.; Miller, R.D. J. Opt. Soc. Am. B, **1996**, *13*, 1713.
29. Stegeman, G.I.; Hall, D.G. J. Opt. Soc. Am., **1990**, *A 7*, 1387.
30. Egami, C.; Suzuki, Y.; Sugihara, O.; Okamoto, N.; Fujiwara, H.; Nakagawa, K.; Fujiwara, H. Appl. Phys. B, **1997**, *64*, 471.
31. Kobolla, H.; Sheridan, J.T.; Gluch, E.; Schwider, J.; Streibl, N. Proc. SPIE, **1992**, *1732*, 278.
32. Wang, X.; Li, L.; Chen, J.; Marturunkakul, S.; Kumar, J.; Tripathy, S.K. Chem. Mater., **1997**, *9*, 45.
33. Wang, X.; Li, L.; Chen, J.; Marturunkakul, S.; Kumar, J.; Tripathy, S.K. Macromolecules **1997**, *30*, 219.
34. Viswanathan, N.K.; Balasubramanian, S.; Li, L.; Kumar, J.; Tripathy, S.K. J. Phys. Chem. B, **1998**, *102*, 6064.